Chemical and oil spill rapid response modelling in the Strait of Gibraltar–Alborán Sea

R. Periáñez

Dpto. Física Aplicada I, E.U. Ingeniería Técnica Agrícola, Universidad de Sevilla, Ctra. Utrera km 1, 41013 Sevilla, Spain

Keywords:
Alborán Sea
Strait of Gibraltar
Numerical modelling
Contaminants
Oil spills Dispersion
Monte Carlo

A B S T R A C T

A numerical model that simulates the dispersion of contaminants, including oil spills, in the Strait of Gibraltar–Alborán Sea region has been developed. The hydrodynamic is solved in advance and includes a barotropic model for calculating tides and a reduced gravity model for the average circulation. Dispersion is calculated using particle-tracking methods. Turbulent diffusion and specific processes for contaminants (for instance decay, biodegradation or oil evaporation) are simulated by Monte Carlo techniques. Computed tide elevations and currents are in agreement with observations. Also, the reduced gravity model reproduces the main characteristics of the residual circulation in the area (namely the western Alborán gyre, WAG, and the coastal circulation mode). Some examples of dispersion calculations are given. The calculated transit time of contaminants over the Alborán Sea is in agreement with that obtained from float experiments. The model may be used to support the decision-making process after a pollutant release in the area.

1. Introduction

Recently, there has been an increasing interest in the development of pollutant dispersion models for the marine environment to use for decision making purposes after contaminant spills. In particular, particle-tracking methods are well suited for problems in which high contamination gradients are involved, since they minimize the effects of numerical diffusion. Also, they can be used to rapidly assess contaminant dispersion if the hydrodynamics are simulated previously off-line. Particle-tracking models have been used to simulate the dispersion of passive tracers (Harms et al., 2000; Gomez-Gesteira et al., 1999), radionuclides (Schonfeld, 1995; Periáñez and Elliott, 2002), oil spills (Proctor et al., 1994; Korotenko et al., 2004) and even contaminated milk (Elliott et al., 2001) in several coastal water environments.

The objective of this work consists of describing a spill model, covering the Strait of Gibraltar and the Alborán Sea, that can be applied to chemical contaminants and oil spills. Due to the water circulation patterns in the area, a spill occurring in the Strait is introduced into the Alborán Sea basin in a time scale ranging from some hours to some days (Echevarría et al., 2002). Thus, the area of the Alborán Sea may be affected by an accident occurring not only inside the Alborán Sea itself, but in the Strait of Gibraltar as well. This work may be considered as the natural continuation of Periáñez (2005a), where a radioactive spill model covering only the Strait of Gibraltar was described. It is a relevant topic due to the intense shipping activities, difficult navigation conditions and ecological and economic value of the area of interest, that will be discussed in some more detail later.

The hydrodynamic is solved in advance. A 2D depth-averaged barotropic model is used to obtain tidalcurrents

E-mail address: rperianez@us.es.

in the region. A reduced gravity model is applied to obtain the average water circulation in the upper water layer, since only spills occurring at the surface will be considered by the moment. Tidal and average circulation are stored in files that will be read by the dispersion code to compute water current at any time and position. Dispersion is solved using a particle tracking method. Thus, the spill is simulated by a number of particles, each of them equivalent to a number of units (for instance mol, kg or Bq), whose paths are followed in time. Specific processes for each contaminant are included in the model using Monte Carlo techniques (radioactive decay, oil evaporation and biodegradation, buoyancy, etc.). Contaminant concentrations may be obtained at the desired time from the density of particles per water volume unit.

Chemical and oil spill dispersion models have been developed and published before in other journals (see for instance references above) and in Ecological Modelling (Nihoul, 1983/1984; Reed et al., 1989; Wong et al., 1989; Jacobi and Schaeffer-Novelli, 1990; Cronk et al., 1990; Carreras and Menéndez, 1990; Periáñez, 1999; Abril et al., 2000; Monte et al., 2006; Jusup et al., 2007; Meyer and Diniz, 2007). These papers describe spill models for freshwater and marine systems and both finite-difference and particle-tracking methods are used. However, this is the first time, to the author knowledge, that a barotropic and a reduced gravity model are coupled to provide the water currents required by a dispersion model of the marine environment. This has been required by the extremely complicated water circulation in the area, which is also the reason why dispersion models have not been described before for this region. The adopted approach, which is described in detail, has proven to be useful when a dispersion model for a region with complex circulation patterns has to be developed.

Some characteristics of the physical oceanography and ecology of the region are briefly described in the next section. The hydrodynamic and dispersion models are next presented. Finally some examples of calculations are given.

2. The Strait of Gibraltar–Alborán Sea region

2.1. *Physical oceanography*

The water circulation in the region is characterized by a surface inflow of Atlantic water and a deep outflow of more dense Mediterranean water. Exchanged flows are (Tsimplis and Bryden, 2000) of the order of 0.7 Sv (1 Sv = 10^6 m^3/s) with a net inflow into the Mediterranean Sea of about 0.05 Sv. This net inflow compensates the excess of evaporation over precipitation and river supply in the Mediterranean. This description of the exchange as a simple two-layer system flowing in opposite directions is a good first approximation (Echevarría et al., 2002). The surface circulation in the Alborán Sea is as follows. The Atlantic water penetrates the Strait of Gibraltar and reaches mean velocities of the order of 0.6 m/s. This water forms a jet that enters the Alborán Sea in a east-northeast direction. The jet flows along the Spanish coast and curves to the south (see map in Fig. 1). Part of it flows to the west, incorporating to an anticyclonic gyre, while the remainder flows to the African coast between Cape Tres Forcas and Alborán Isle

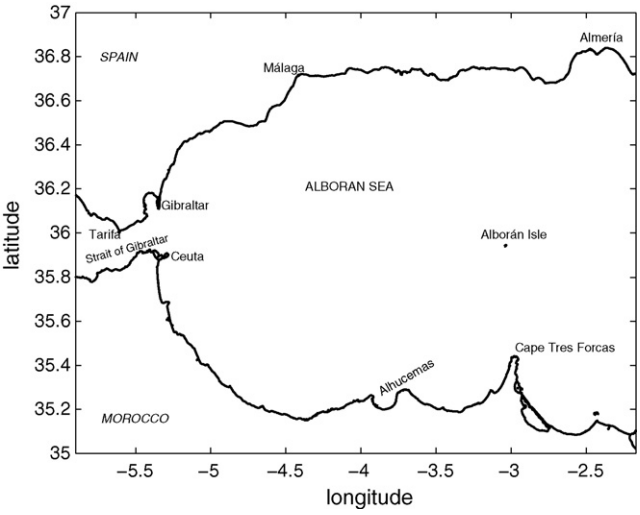

Fig. 1 – Map of the Strait of Gibraltar and Alborán Sea.

(Perkins et al., 1990). This is known as the Western Alborán Gyre (WAG). Another gyre, more elusive, fills the eastern basin of the Alborán Sea: it is the Eastern Alborán Gyre (EAG), that is out of domain of our model. A detailed description may be seen for instance in Vargas-Yáñez et al. (2002), Vélez-Belchí et al. (2005) and references cited in these works, which include the classical works carried out since the 1970s.

The WAG fills the western Alborán Sea between the Strait of Gibraltar and the Alborán Isle, thus extending some 200 km in the west-east direction. It extends towards the south, reaching the coast of Morocco (Perkins et al., 1990; Werner et al., 1988). The vertical scale of the gyre is about 200 m. It has also been suggested (Preller, 1986) that a coastal feature (Cape Tres Forcas) acts as a barrier to the gyre growth. The variability of circulation in the Alborán Sea has been investigated by Vargas-Yáñez et al. (2002). These authors conclude, from their results and from the revision of previous works, that the WAG is the dominant circulation pattern in summer and the coastal mode is more likely in winter. In this coastal mode, the Atlantic current flows close to the African coast once it exits the Strait of Gibraltar and no gyre is apparent. Nevertheless, it has to be clearly pointed out that this bimodal behaviour is not perfectly defined, as can be seen for instance in the data presented in Heburn and La Violette (1990). In fact, there are transitions between the two commented behaviours (Vázquez-Cuervo et al., 1996; Vélez-Belchí et al., 2005 and references here included). In this work, the presence of the WAG and the coastal model will be sometimes referred as the usual summer and winter conditions, respectively. However, it must be kept in mind that an absolutely clear annual cycle does not exist.

With respect to the tides in the area, an important feature of the tidal flow in the Strait is that it can be considered, as a first approach, as barotropic. Indeed, 93% of the variance of current velocity in the semidiurnal band has a barotropic character in the Strait (Mañanes et al., 1998). Tsimplis and Bryden (2000) have pointed out that tidal currents are barotropic and larger than the mean inflow or outflow. The semidiurnal tide dominates ADCP records (acoustic doppler current profiler) in the

Strait, obscuring the expected two-layer character of the mean flow. The tidal signal is so strong that it reverses the currents near the bottom for a part of each tidal cycle. As a consequence, 2D depth-averaged models have already been applied to simulate surface tides in the Strait (Tejedor et al., 1999). Tsimplis et al. (1995) have even used a 2D barotropic model for simulating tides in the whole Mediterranean Sea. The success of these models indicates that the baroclinic component is of secondary importance.

In the case of the main tidal constituent, M_2, tide amplitude at the Atlantic entrance of the Strait is about 0.8 m. This amplitude decreases towards the east. Thus, at the Mediterranean entrance is only about 0.3 m. The amplitude of the tide is reduced more in the Alborán Sea, reaching 0.09 m at the east limit of our domain (see map in Fig. 1). The associated currents decrease in a similar way: from tidal currents of the order of 1 m/s in the Strait to currents of a few cm/s in the Alborán Sea basin. Similar behaviour is observed for the S_2 constituent.

From this analysis it seems evident that tides are relevant, for the transport of pollutants in water, in the area of the Strait of Gibraltar. However, once that pollutants enter the Alborán Sea the main mechanism is transport by the residual (average) circulation. Contaminants may remain trapped in the WAG, and an appropriate description of this average circulation is thus required for a realistic calculation of contaminant dispersion.

2.2. *Ecology and shipping activities*

The Strait of Gibraltar and the Alborán Sea are the only connection between the Mediterranean Sea and the Atlantic Ocean. As a consequence, there is an intense traffic of merchant vessels: over 70,000 per year, 30% of them declaring hazardous cargos. Traffic of oil tankers is about 5000 vessels per year. Also, over 12,000 vessels, mostly passenger ferries, cross the Strait each year between the south and north coasts (Nav42, 1998). Connections between the towns of Málaga and Almería (Spain) and the north African coast must be added (see Fig. 1 for locations). Fishing activities must finally be added. Algeciras is the most important port in Spain (and number 25 in the world), with 65.7 Mt of cargo handled in 2004 (Autoridad Portuaria de la Bahía de Algeciras, 2006). Fishing vessels operating from this port are 347.

It is usual to have adverse meteorological conditions in the Alborán Sea and, mainly, in the Strait, with more than 54% of days of moderate to poor visibility and 13% of days with persistent fog conditions (Nav42, 1998). Winds must be added, with frequent east and west gales. East winds (*levantes*) blow an average of 165 days per year, predominantly from April to October, with an average speed of the order of 50 km/h. Maximum speed reaches 125 km/h. Gusts of winds can remain up to 7–10 days. West winds (*ponientes*) blow an average of 60 days per year, from November to March predominantly. Minimum and maximum speeds are 30 and 90 km/h. West winds are not as persistent as *levantes*, lasting for some 12–36 h.

The particular conditions in the area (intense traffic and adverse meteorology) make navigation difficult. Indeed, 81 accidents have occurred in the Strait (Nav42, 1998) in the last years, with 14 collisions and 16 groundings. For instance, in 1990 there was a collision between the oil tanker Hesperus and the chemical tanker Sea Spirit. More recently, a ferry and a gas tanker collided off Ceuta.

This region has a high ecological value, being essential in marine and aerial migratory processes. By decree 57/2003 (4 March 2003) of the Junta de Andalucía, the Natural Park of Algeciras-Tarifa Coast was created. It consists of 191.3 km^2, 92.47 of which correspond to the marine part of the Park. A review about geomorphology, flora and fauna of the Park may be consulted in Cabello (2003), but some data are summarized here. Over 1900 species of marine flora and fauna living in the Park have been described. Some of the species with a major interest (due to their endemic character and/or rareness) are sponges like *Axinella estacioi* and jellyfishes (like *Merona ibera*, *Cervera atlantica* and *Scleranthelia microsclera*). There are other 23 species under strict conservation, like *Patella ferruginea* (the largest limpet of European coasts), *Lithophaga lithophaga*, *Pinna nobilis*, *Centrostephanus longispinus*, *Astroides calicularis*, etc. As the connection between the Mediterranean Sea and the Atlantic Ocean, marine turtles and mammals (dolphin, porpoise, sperm whale, killer whale) travel through the area.

Finally, the region has a high tourist interest, since many kilometers of sand beaches in the area of the Strait and the Costa del Sol (Málaga) attract thousands of tourists each year. There are also some important towns. A release of contamination in the area as a consequence of an accident (or a deliberate release) can lead to relevant ecological and economic impacts.

3. Model description

The hydrodynamic models (barotropic and reduced-gravity models for tides and residual circulation, respectively) are described first. Next, the dispersion particle tracking model is presented.

3.1. *2D depth-averaged barotropic model*

As commented before, this model is used to simulate tides in the domain of interest. The depth-averaged hydrodynamic equations may be written as (Periáñez, 2005b):

$$\frac{\partial z}{\partial t} + \frac{\partial}{\partial x}(Hu) + \frac{\partial}{\partial y}(Hv) = 0 \tag{1}$$

$$\frac{\partial u}{\partial t} + u\frac{\partial u}{\partial x} + v\frac{\partial u}{\partial y} + g\frac{\partial z}{\partial x} - \Omega v + \frac{\tau_u}{\rho H} = A\left(\frac{\partial^2 u}{\partial x^2} + \frac{\partial^2 u}{\partial y^2}\right) \tag{2}$$

$$\frac{\partial v}{\partial t} + u\frac{\partial v}{\partial x} + v\frac{\partial v}{\partial y} + g\frac{\partial z}{\partial y} + \Omega u + \frac{\tau_v}{\rho H} = A\left(\frac{\partial^2 v}{\partial x^2} + \frac{\partial^2 v}{\partial y^2}\right) \tag{3}$$

where u and v are the depth averaged water velocities along the x and y axes, D the depth of water below the mean sea level, z the displacement of the water surface above the mean sea level measured upwards, $H = D + z$ the total water depth, Ω the Coriolis parameter ($\Omega = 2w \sin\beta$, where w is the earth rotational angular velocity and β is latitude), g acceleration due to gravity, ρ water density and A is the horizontal eddy viscosity. τ_u and τ_v are friction stresses that are written in terms of

a quadratic law:

$$\tau_u = k\rho u\sqrt{u^2+v^2}, \qquad \tau_v = k\rho v\sqrt{u^2+v^2} \tag{4}$$

where k is the bed friction coefficient.

The solution of these equations provides the water currents at each point in the model domain and for each time step. Currents are treated through standard tidal analysis and tidal constants are stored in files that will be read by the dispersion code to calculate the advective transport of particles. The model includes the two main tidal constituents, M_2 and S_2. Thus, the hydrodynamic equations are solved for each constituent and tidal analysis is also carried out for each constituent separately.

Some open boundary conditions must be provided. Surface elevations are specified, from observations, along open boundaries of the computational domain. A radiation condition is applied to the water velocity component that is normal to the open boundary:

$$\frac{\partial\phi}{\partial t} = c\frac{\partial\phi}{\partial n} \tag{5}$$

where ϕ is the current component normal to the boundary, in the direction n, and c is a phase speed calculated as in Jensen (1998). Water flux across a land boundary is set to zero as usual.

Equations are solved using a explicit finite difference scheme (Periáñez, 2005b). The computational domain extends from 35°00′ N to 36°56′ N and from 5°54′ W to 2°10′W. Resolution of the grid is 2 min, that is equivalent to $\Delta x = 2972$ m and $\Delta y = 3341$ m. Water depths were downloaded from the NOAA Geodas database. Time step, limited by the CFL (Courant–Friederichs–Lewy) stability condition is $\Delta t = 10$ s. Once a stable periodic solution is achieved, tidal analysis is carried out to determine tidal constants that are used by the particle-tracking code.

3.2. *Reduced-gravity model*

Essentially it is a two-layer model in which the lower layer is infinitely deep and at rest. Thus, the interface between the two layers may deform without any resulting motion in the lower layer. In spite of this relative simplicity, reduced gravity models are used at present to study different problems in oceanography (Cummins and Lagerloef, 2004; Chern and Wang, 2005; Morales-Maqueda et al., 1999; Arruda et al., 2004).

Equations are expressed in the following way (Kowalick and Murty, 1993):

$$\frac{\partial h}{\partial t} + \frac{\partial hu}{\partial x} + \frac{\partial hv}{\partial y} = 0 \tag{6}$$

$$\frac{\partial u}{\partial t} + u\frac{\partial u}{\partial x} + v\frac{\partial u}{\partial y} + g'\frac{\partial h}{\partial x} - \Omega v + \frac{\tau_u}{\rho_1 h} = A\left(\frac{\partial^2 u}{\partial x^2} + \frac{\partial^2 u}{\partial y^2}\right) \tag{7}$$

$$\frac{\partial v}{\partial t} + u\frac{\partial v}{\partial x} + v\frac{\partial v}{\partial y} + g'\frac{\partial h}{\partial y} + \Omega u + \frac{\tau_v}{\rho_1 h} = A\left(\frac{\partial^2 v}{\partial x^2} + \frac{\partial^2 v}{\partial y^2}\right) \tag{8}$$

where h is the thickness of the upper layer and g' is the reduced gravity, written as:

$$g' = g\frac{\Delta\rho}{\rho_2} \tag{9}$$

In this equation $\Delta\rho = \rho_2 - \rho_1$ is the density difference between the lower and upper layer. Friction between both water layers is described by a quadratic law, as in the barotropic model:

$$\tau_u = k\rho_1 u\sqrt{u^2+v^2}, \qquad \tau_v = k\rho_1 v\sqrt{u^2+v^2} \tag{10}$$

where k is the friction coefficient. The same numerical scheme as in the barotropic model was used to solve the reduced gravity equations. One restriction of layered models is that when the topography intersects the interface the solution becomes inestable (Preller, 1986). To avoid this, the topography of the Alborán Sea was restricted to a minimum of 350 m. The downloaded bathymetry was artificially modified to describe the Alborán Isle as approximately 20 km × 10 km (the island disappears if minimum depth is restricted to 350 m due to the limited resolution of the downloaded data). These dimensions are a good estimate of the island size at 200 m depth. Such modification was also carried out in a previous study (Preller, 1986) to include the shallow topography associated with the island.

The CFL condition is less restrictive in this case than in the barotropic model since now g is replaced by the reduced gravity g'. Thus time step for the explicit integration is increased to $\Delta t = 800$ s. The model is integrated specifying water currents along the open western boundary until a stable solution is achieved. The computed steady current and upper layer thickness over the domain are stored in files that will be read by the dispersion code. Radiation boundary conditions are used along the open eastern boundary.

Two average water circulation patterns have been obtained with the reduced gravity model: one corresponding to the usual summer situation (existence of the gyre) and the other one corresponding to the usual winter situation (coastal circulation). As will be discussed in some more detail below, different circulation patterns are obtained changing the u component of the water current across the open western boundary.

3.3. *Particle-tracking dispersion model*

In particle-tracking models a contamination release is simulated by a number of particles, each one of them equivalent to a number of units. The path followed by each particle is then calculated. Contaminant concentrations may be calculated at the desired time from the density of particles per water volume unit. Specific processes for each contaminant have to be described adequately.

Advection is computed solving the following equation for each particle:

$$\frac{d\mathbf{r}}{dt} = \mathbf{q} \tag{11}$$

where $\mathbf{r}$ is the position vector of the particle and $\mathbf{q}$ is the current vector (due to tides plus residual circulation) solved in components u and v. The particle-tracking model is three-dimensional, but the hydrodynamic calculations provide depth-averaged currents. In the main body of water above the logarithmic layer, the flow gradually increases in a manner which may be represented as (Pugh, 1987):

$$u_{z'} = u_s \left(\frac{D - z'}{D} \right)^{1/m} \tag{12}$$

where $u_{z'}$ is the current speed at a level z' below the sea surface and u_s is the surface flow. From observations, it has been deduced that m ranges between 5 and 7. The surface current can be deduced from the depth averaged one (Pugh, 1987):

$$u_s = \frac{m+1}{m} \bar{u} \tag{13}$$

where $\bar{u}$ is the depth averaged current. Thus, components u and v of the current at any depth can be obtained from their depth-averaged values (provided by the hydrodynamic model) applying Eqs. (12) and (13). This current profile has already been used (Riddle, 1998) in particle tracking calculations. The total water depth is replaced by the thickness of the upper water layer in the case of the residual current, provided by the reduced gravity model. Actual water depth, however, is used to obtain the profiles of tidal currents, since they are obtained from a barotropic model in which the complete water column is considered.

Wind is typically included in particle-tracking models assuming that the surface wind-induced current is 3% of the wind speed measured 10 m above the sea surface (Pugh, 1987; Proctor et al., 1994). This current decreases logarithmically to zero at a depth z_1, that is assumed to be 20 m (Elliott, 1986). The wind induced current at any depth may thus be written as (Pugh, 1987):

$$u_{z'} = \begin{cases} u_0 - \dfrac{u^*}{\kappa} \ln \left(\dfrac{z'}{z_0} \right) & \text{if} \quad z' < z_1 \\ 0 & \text{if} \quad z' \geq z_1 \end{cases} \tag{14}$$

where u_0 is the surface wind-induced current, $\kappa = 0.4$ the von Karman constant, u^* a friction velocity and z_0 is the sea surface roughness length, which has values between 0.5 and 1.5 mm. It has been obtained (Pugh, 1987) that the friction velocity can be estimated as

$$u^* = 0.0012W \tag{15}$$

for a wide range of conditions, where W is wind speed 10 m above the sea surface. From these equations, the wind effect on the advection of particles can be calculated. Of course, the current profile is solved in the u and v components.

Three-dimensional diffusion is simulated using a random walk method (Proctor et al., 1994; Periáñez and Elliott, 2002). It has been shown that it is a simulator of Fickian diffusion provided that the maximum sizes of the horizontal and vertical steps, D_h and D_v, respectively, are:

$$D_h = \sqrt{12 K_h \Delta t}, \qquad D_v = \sqrt{2 K_v \Delta t} \tag{16}$$

where K_h and K_v are the horizontal and vertical diffusion coefficients, respectively.

Decay of particles is also included (this is relevant for instance in the case of radioactive discharges) using a stochastic method, as usually in particle-tracking models (Proctor et al., 1994; Periáñez and Elliott, 2002).

The adsorption of pollutants by suspended and bottom sediments can also be simulated with a particle-tracking model (Periáñez and Elliott, 2002). However, these processes are neglected in the present study since suspended matter concentrations are very low in the area, typically 0.1–0.5 mg/L (León-Vintró et al., 1999). Also, since the pycnocline is acting as a barrier for vertical mixing, interactions of pollutants with bed sediments can be neglected.

Specific processes affecting oil spills have to be included. Thus, oil droplets have a size distribution so that larger ones tend to remain in the water surface. Smaller droplets mix downwards because of turbulence and shear diffusion results in a patch elongated in the current direction. The model also includes the effects of surface evaporation of oil and decomposition within the water column (for instance because of biodegradation).

The buoyancy force depends on the density and size of droplets. The rise velocity, w, can be described as (Proctor et al., 1994):

$$w = \frac{g d^2 ((1 - \rho_0)/\rho)}{18 \nu} \tag{17}$$

for small droplets with diameter $d \leq d_c$ (laminar motion). In this equation ρ and ρ_0 are the densities of water and oil, respectively and ν is the water kinematic viscosity. For large droplets with $d > d_c$ (turbulent motion) the rise velocity is:

$$w = \left(\frac{8}{3} g d ((1 - \rho_0)/\rho) \right)^{1/2} \tag{18}$$

The critical diameter, d_c, is given by the expression

$$d_c = \frac{9.52 \nu^{2/3}}{g^{1/3} ((1 - \rho_0)/\rho)^{1/3}} \tag{19}$$

that is deduced matching the Reynolds numbers at which the transition from laminar to turbulent flow occurs.

The diameter of each oil droplet in the simulation is assigned randomly between a minimum and maximum diameter, $d_{min} - d_{max}$.

The effects of oil evaporation and decomposition are treated in a similar way as radioactive decay and are defined by the corresponding e-folding times. Different values are used for evaporation, T_{ev}, and decomposition, T_{de}. Additionally, only particles within a depth $z_{ev} = 0.25$ m below the surface can be evaporated, whereas droplets at any depth can experience decomposition (Proctor et al., 1994). Typical values for these parameters will be given below.

If during a computation an oil droplet reaches the coastline, it is considered *beached*. Thus, the droplet stays in the coast without moving any more.

Values for the diffusion coefficients have to be provided. The horizontal diffusion coefficient depends on the horizontal

grid spacing. Following Dick and Schonfeld (1996):

$$K_h = 0.2055 \times 10^{-3} \Delta x^{1.15} \quad (20)$$

The present grid resolution gives $K_h = 2.0\,m^2/s$. For the vertical diffusion coefficient a typical value of $0.001\,m^2/s$ is used (Elliott et al., 2001; Dick and Schonfeld, 1996).

There is no stability criterion equivalent to the CFL condition in the particle tracking calculations, although it is wise to ensure that each particle does not move through a distance that exceeds the grid spacing during each time step. Thus, time step was fixed as $\Delta t = 300\,s$.

3.4. *Computational scheme*

The dispersion code automatically reads six files which contain the topography of the Alborán Sea, amplitudes and phases of the two tidal constituents included in the model (M_2 and S_2), and the residual circulation (for WAG or coastal circulation modes). These files are provided by the hydrodynamic module that has been run off-line, as noted before. The user must also include some information for each simulation, related to the release characteristics. This information is summarized in Table 1. In particular, date and time of the discharge (and duration in the case of continuous releases) must be given. Thus, the appropriate phase of each tidal constituent at $t = 0$ must be specified. The values used in this model correspond to the origin of time being 1 January 2003 at 0:15 h Greenwich time. Wind conditions are also defined in a file that must be edited before running the model. Variable winds can be included.

Table 1 – Information required by the model to be introduced by the user

Release point coordinates
Select instantaneous/continuous release option
Wind file name
Select circulation mode (gyre/coastal)
Release date (day, month, year)
Release time, UTC, (h, min)
Residual current modulator
Simulation time (days)
Magnitude of the release in the corresponding units
Contaminant decay constant (radioactive)
Oil spill additional information
Oil density
Droplet minimum and maximum sizes
e-folding times (evaporation and decomposition)

The reduced gravity model provides the residual current in the domain, as already noted. Nevertheless, residual currents are controlled by the water inflow through the Strait of Gibraltar that, as will be discussed in some more detail below, presents some variability. Thus, a factor that acts as a modulator of the residual current amplitude must be introduced. If 1 is used, the residual current for the average water inflow (for WAG or coastal modes) through the Strait is used in the calculations. These average currents may be slightly amplified or reduced by specifying values for the modulator larger or smaller than 1, respectively.

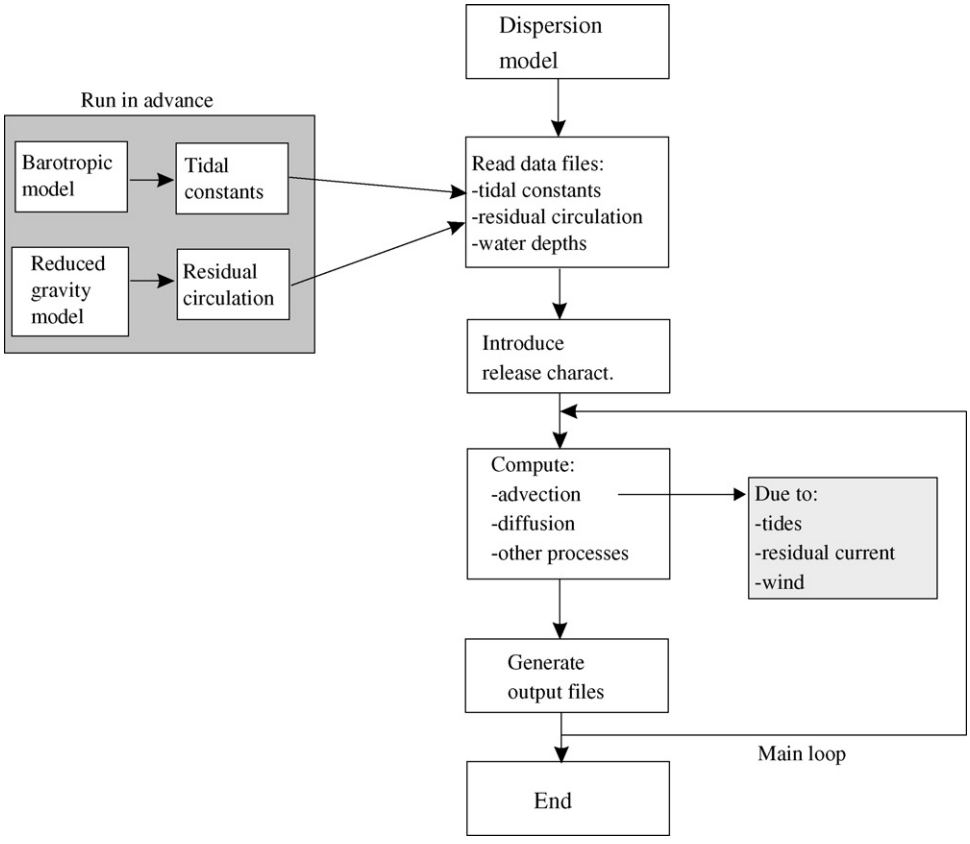

Fig. 2 – Flow diagram of the computation process in the model.

The model provides several output files. It gives the coordinates of each particle at several times during the simulation. Thus, snap shots of particles can be drown to study the evolution of the discharge along time. In particular, 12 snaps shots at constant intervals along the simulation are provided. Another file contains a map of the final contaminant concentration over the domain computed from the density of particles per water volume unit. Optionally, the time evolution of pollutant concentrations at desired points over the domain can be obtained.

A simplified flow diagram of the whole computation process is shown in Fig. 2. The hydrodynamic is solved in advance and files generated are used by the dispersion model to calculate the currents at any position of the domain for each time step.

4. Results and discussion

Results of the hydrodynamic models are presented first. Next, some examples of dispersion calculations are given.

4.1. *Hydrodynamics*

Computed values of the amplitude and phase of the water surface elevation produced by the M_2 and S_2 tides have been compared with observed values (Tsimplis et al., 1995; Manzella and Elliott, 1991) at different locations in the Strait of Gibraltar and the Alborán Sea. Results are given in Table 2. Locations may be seen in the map in Fig. 1. It can be observed that generally there is a good agreement between the measured and computed tidal constants for both constituents.

A tidal chart for the M_2 tide is shown in Fig. 3. The same color joins points with the same tide amplitude (corange chart). The amplitude decreases quickly in the Strait of Gibraltar, from some 0.75 m in the Atlantic entrance to 0.30 in the section of Gibraltar. There is a further, although slower, amplitude reduction in the Alborán Sea, reaching only some 0.10 m at the eastern boundary. It can be seen that corange lines are oriented in a south-north direction, while cotidal lines (join points with the same tidal phase; not shown) are essentially in a northeast direction, in agreement with observations and the earlier computations in Tsimplis et al. (1995).

The spatial distribution of the M_2 current amplitude is presented in Fig. 4 as an example. This distribution is in good agreement with that presented in Tsimplis et al. (1995). The current amplitude in most of the Alborán Sea is some 0.03 m/s.

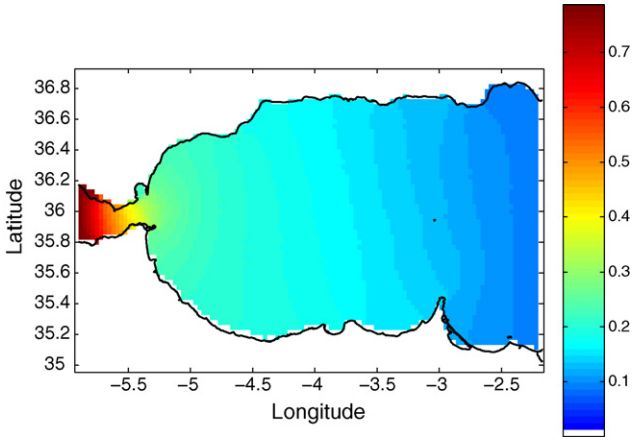

Fig. 3 – Corange chart for the M_2 tide. Amplitude of the tide is given in m.

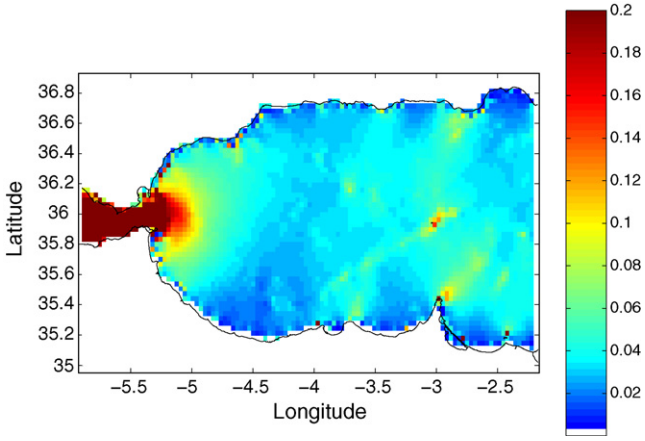

Fig. 4 – Current amplitudes (m/s) for the M_2 tide.

Only in some specific areas larger currents are obtained. This is the case of the south-north section going from Cape Tres Forcas to Alborán Isle and the Spanish coast. Currents of the order of 0.06–0.09 m/s are computed close to the Cape, around Alborán Isle and close to the Spanish coast. This is in good agreement with the earlier computations presented in Tsimplis et al. (1995). Current amplitude increases as approaching Gibraltar Strait, where, as expected, maximum values are obtained. Indeed, currents of the order of 0.8 m/s are computed in some locations. For clarity reasons, however, the

Table 2 – Observed and computed amplitudes (A, cm) and phases (g, deg) of tidal elevations at several locations indicated in Fig. 1

Station	M_2				S_2			
	A_{obs}	g_{obs}	A_{comp}	g_{comp}	A_{obs}	g_{obs}	A_{comp}	g_{comp}
Tarifa	42	57	41	45	14	85	16	79
Ceuta	30	50	32	52	11	76	12	86
Málaga	17	59	18	42	7	72	8	77
Alhucemas	18	58	18	56	7	80	7	89
Almería	9	51	9	49	4	78	4	77
Gibraltar	30	46	29	41	11	72	12	77

scale maximum in Fig. 4 is limited to 0.2 m/s. In the case of the S_2 tide, results show a similar decrease in the tide amplitude, from some 0.25 m at the Atlantic entrance of the Strait to some 0.04 m at the eastern open boundary of the domain. Current amplitudes decrease from maximum values of the order of 0.25 m/s in the Strait of Gibraltar to currents weaker than 1 cm/s in the Alborán Sea.

Residual currents provided by the reduced gravity model are presented in Fig. 5 for both summer and winter usual conditions (existence of the WAG and coastal mode, respectively). The different situations are obtained simply changing the inflow through the Strait of Gibraltar. The collapse of the WAG may be related to its westward advection, that is caused by an enhanced transport towards the Atlantic in the deep water layer (Heburn and La Violette, 1990). Other authors agree that the collapse of the WAG is related to minimum inflow through the Strait of Gibraltar (Béranguer et al., 2005). Nevertheless, another proposed mechanism for the WAG collapse is its migration to the east (Vélez-Belchí et al., 2005). In this case, a decrease in the Atlantic inflow is required after an initial increase of water velocity in the Strait of Gibraltar to allow the eastward migration of the gyre. Nevertheless, other different mechanisms have been proposed to explain WAG disappearances (see discussion in Vélez-Belchí et al., 2005).

When the WAG is present, the jet of Atlantic water entering through the Strait of Gibraltar flows towards the east along the Spanish coast and partially curves to the south before reaching Alborán Island. Part of this flow continues to the east between Cap Tres Forcas and Alborán Island and the remaining rotates towards the west, flowing along the African coast. A gyre of anticyclonic circulation is thus completed (Fig. 5). During the coastal circulation mode, the Atlantic current flows close to the African coast once it exits the Strait of Gibraltar. These circulation patterns are in good qualitative agreement with those deduced from satellite thermal images shown in Vargas-Yáñez et al. (2002).

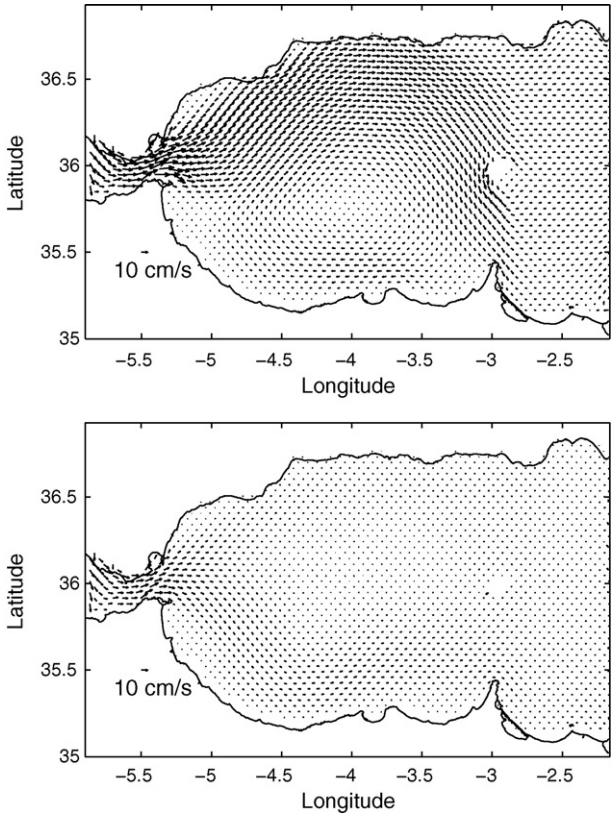

Fig. 5 – Steady currents computed with the reduced gravity model for summer (up) and winter (down) usual conditions. Only 50% of the computed vectors are drawn.

The computed inflow through the Strait of Gibraltar is 0.86 and 0.54 Sv when the WAG is present and for the coastal mode, respectively. Current-meter observations and recent models give a transport of about 0.8 Sv (Béranguer et al., 2005). In particular, Tsimplis and Bryden (2000) gave an estimation of 0.66 ± 0.47 Sv for the average inflow, where the large error is due to seasonal variability. Our results are in agreement with this estimate. Nevertheless, flows during winter and summer are affected by other factors as for instance atmospheric pressure differences between the Atlantic and the Mediterranean. Thus, the residual current modulator is introduced to be able to account for this variability.

It seems that, generally speaking, the present model gives a representation of the system that is realistic enough to implement on it the particle-tracking dispersion code. Some examples of dispersion calculations will be presented now.

4.2. *Dispersion*

Chemical spills will be considered first. Some experiments with instantaneous discharges have been carried out. It has been assumed that releases occurred in all cases in 1 July 2005 at 0:00 h UTC (just as an example of usual summer conditions, there is not any particular reason to select this date and time). No wind is considered and the decay constant is set to zero (stable chemical pollutant). The total pollutant discharged is 1×10^{12} units. Finally, the current amplitude modulator is 1 (average inflow through the Strait of Gibraltar).

In the first experiment, the fate of a release occurring at the centre of the Strait of Gibraltar (coordinates 35.98°, −5.57°) has been simulated. In this case the patch is introduced in the Alborán Sea by the Atlantic water jet and moves rapidly towards the east, in a trajectory that is initially parallel to the Spanish coast. Then curves to the south and the patch is divided by Alborán Island. The time required by the patch to reach the east boundary of the domain is of some 50 days, which implies an average velocity of the order of 9 cm/s. Three of the 12 snapshots produced by the model are shown in Fig. 6 as an example. The 25 days elapsed between the first and third snapshots are in agreement with the also 25 days taken by two neutrally buoyant Lagrangian floats, launched at meridian −4.88° (latitude 36.1°), to reach the passage between Cape Tres Forcas and Alborán Island (Vélez-Belchí et al., 2005). If the same experiment is repeated at a short temporal scale, simulating only the first 4 days, then the snapshots produced by the model show how the patch moves in the Strait forward and backwards because of tidal oscillations. These movements cannot be appreciated in longer simulations due to the longer time elapsed between snapshots.

Another experiment consisted of simulating an accident in the central part of Alborán Sea (coordinates 35.98°, −4.09°). Now all particles remain trapped in the WAG. Indeed, the time

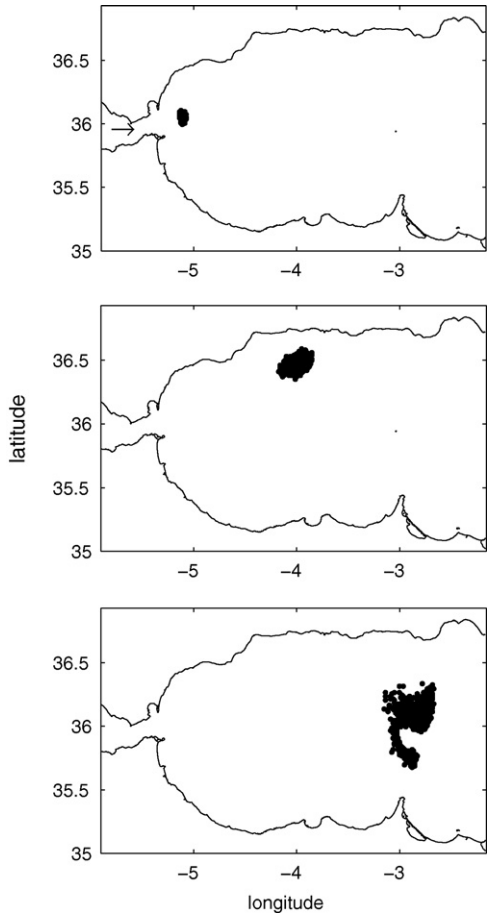

Fig. 6 – Snapshots showing the position of particles 2.5 (up), 12.5 (middle) and 27.5 (down) days after an instantaneous release of a stable chemical contaminant in the central part of the Strait (arrow position).

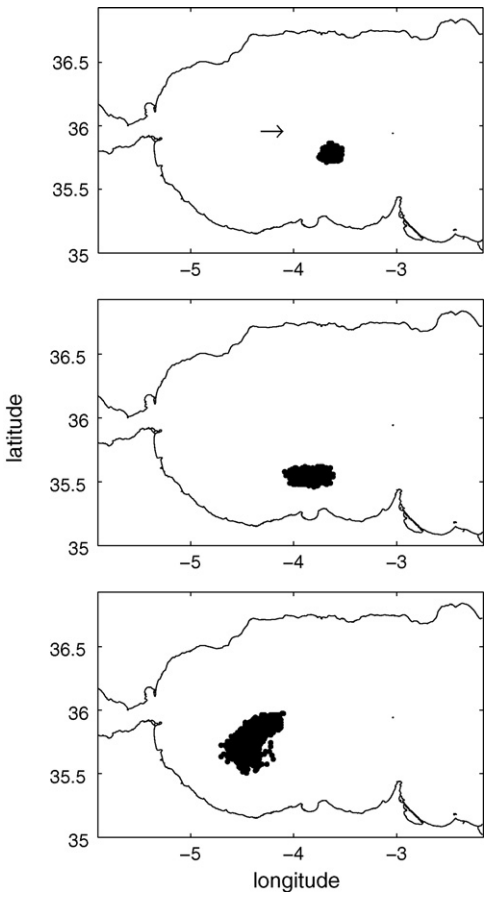

Fig. 7 – Snapshots showing the position of particles 15 (up), 30 (middle) and 55 (down) days after an instantaneous release of a stable chemical contaminant in the central part of the Alborán Sea at the arrow position.

required to complete a loop is of the order of 60 days. Some results may be seen in Fig. 7, where the anticyclonic rotation of the patch can be observed. As an example, the map of concentrations, computed from the density of particles per water volume unit, is presented in Fig. 8.

Some examples of model results in the case of oil spills are presented now. Values for the parameters required by the oil spill model must be set first. Oil density typically ranges from 660 kg/m^{3}in the case of paraffin to 1200 kg/m^3 in the case of aromatic (poli-cyclic) and naphtheno-aromatic oils (Korotenko et al., 2004). A density equal to 900 kg/m^{3}will be used in the simulations, that is between the value 870 kg/m^{3}used in some calculations carried out for the Arabian Gulf spills of 1991 (Proctor et al., 1994), and the value 950 kg/m^{3}used in some hypothetical oil spill simulations for the Irish Sea (Elliott, 2004).

The oil droplet size is assumed to be in the range 60–600 μm, that are typical values (Proctor et al., 1994; Elliott, 2004; Korotenko et al., 2004). The same values for the oil e-folding times as in Proctor et al. (1994) have been used: 25 and 250 h for evaporation and decomposition, respectively.

An example of results is presented in Fig. 9, that also illustrates the case of a continuous release. In this case, the accident originates an oil spill off the harbour of Gibraltar (coordinates 36.14°, −5.34°) again at 0:00 h on 1 July 2005. The release lasts for 5 days and the movement of oil droplets is computed during 30 days. A very elongated patch, in the direction of the mean current, that travels along the Spanish coast is observed. As can be seen in the lowest panel of Fig. 9, the

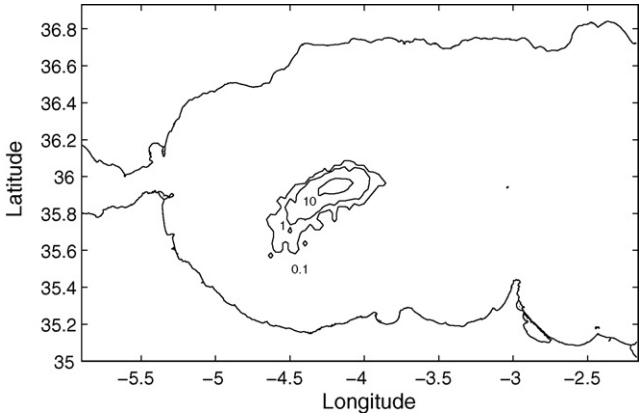

Fig. 8 – Concentration map (units/m^3) obtained 60 days after the release in Fig. 7.

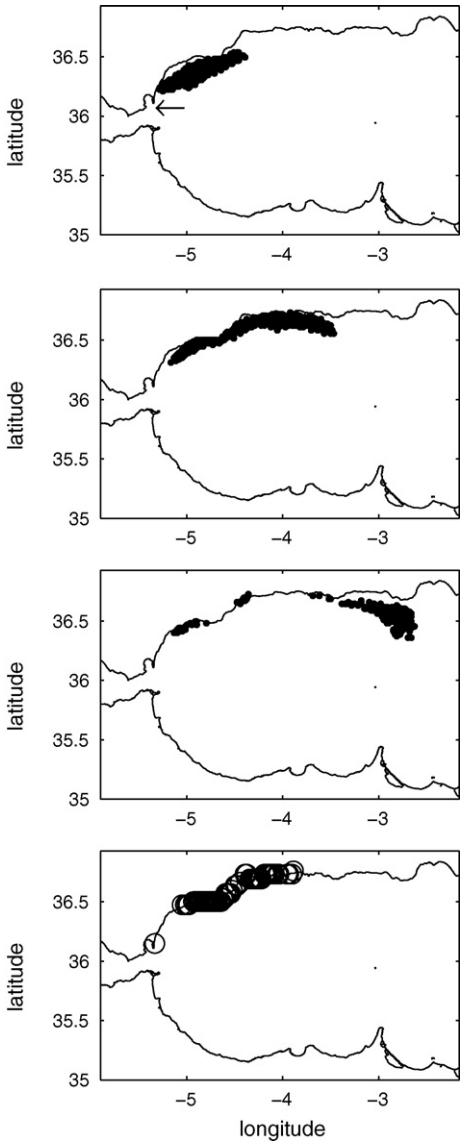

Fig. 9 – Snapshots showing the position of particles 7.5, 15 and 27.5 (from top to bottom) days after an oil release occurring off Gibraltar port at the arrow position. Circles in the lowest panel show particles that have been beached during the simulation.

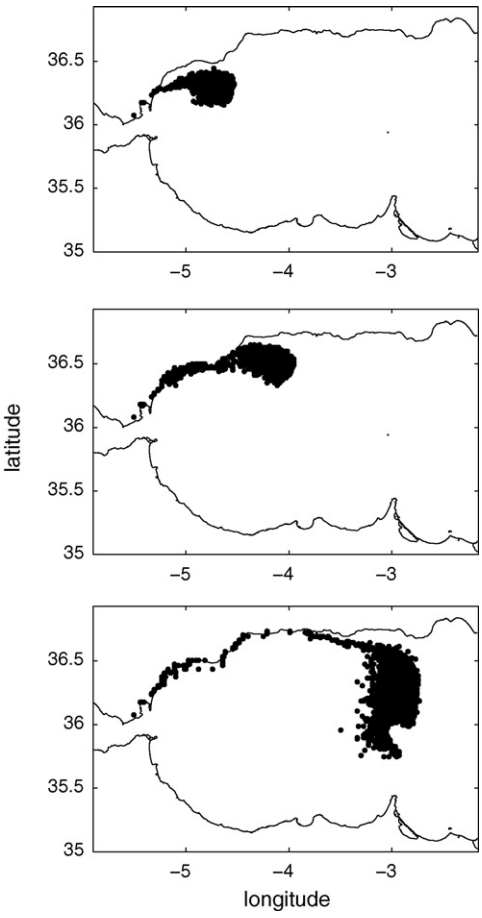

Fig. 10 – Snapshots showing the position of particles 7.5 (up), 12.5 (middle) and 27.5 (down) days after an instantaneous release of a stable chemical contaminant in the central part of the Strait. A 10 m/s wind blowing from the east is included.

coast is contaminated from −5° to −4°, in longitude, approximately. The area of Gibraltar is contaminated as well. During the 5 days of release the total number of particles that are introduced is 36,000, at a rate of 25 new particles each time step. Only 215 remain in water and 520 are beached after one month. This implies that 1.4% of the released oil has reached the coast and that 0.6% is still being transported by water. The remaining oil has decayed or has been evaporated.

The effects of winds will be illustrated in what follows. The simulation shown in Fig. 6(stable chemical pollutant release occurring at the central part of the Strait of Gibraltar) has been repeated but with a 10 m/s wind blowing from the east. Results are presented in Fig. 10. If this is compared with Fig. 6, it can be seen that the wind tends to retain the contamination inside the Alborán Sea for a longer time. Also, a tail of particles is produced along the Spanish coast where some contamination is retained. Thus, this region would remain contaminated for a longer time as a consequence of the wind. Finally, it can also be seen that more intense mixing of contamination along a south-north direction is produced than under calm conditions. West winds, in the same direction as the average currents, produce the opposed effect: a faster contaminant flushing off from the region. It must be pointed out that it is not realistic to have these wind conditions persisting without change during such a long time. However, the aim of the experiment is simply to show the effect of winds on the behaviour of the contamination patch. As has been commented before, the model may anyway deal with non-constant wind fields.

As another example of the results that may be obtained with the model, the time evolution of the number of particles at point with coordinates 36.47°, −4.58°, that is located close to the town of Málaga, in the Spanish coast, is presented in Fig. 11 for the same experiment (east wind). It can be seen that contamination arrives 200 h after the accident and that the maximum number of particles (thus maximum concentration) is obtained after 232 h. The patch completely crosses after 278 h. Since in an instantaneous release simulation 3000 parti-

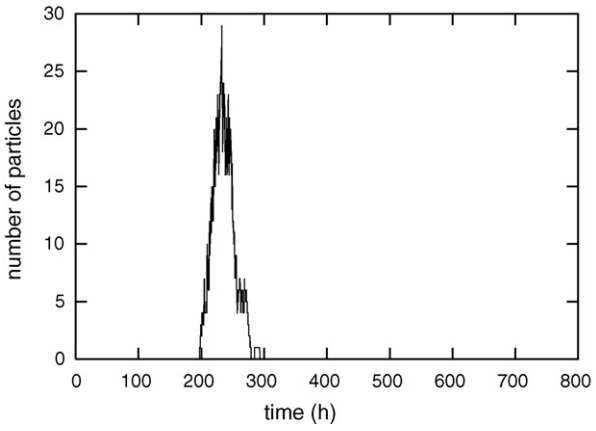

Fig. 11 – Time evolution of the number of particles at point with coordinates 36.47°, −4.58° for the east wind experiment (Fig. 10).

cles are used and the total amount of contaminant released is 1×10^{12} units, each particle corresponds to 3.3×10^{8} units. The maximum number of particles is 29, that implies a maximum concentration equal to 6.7 units/m^3.

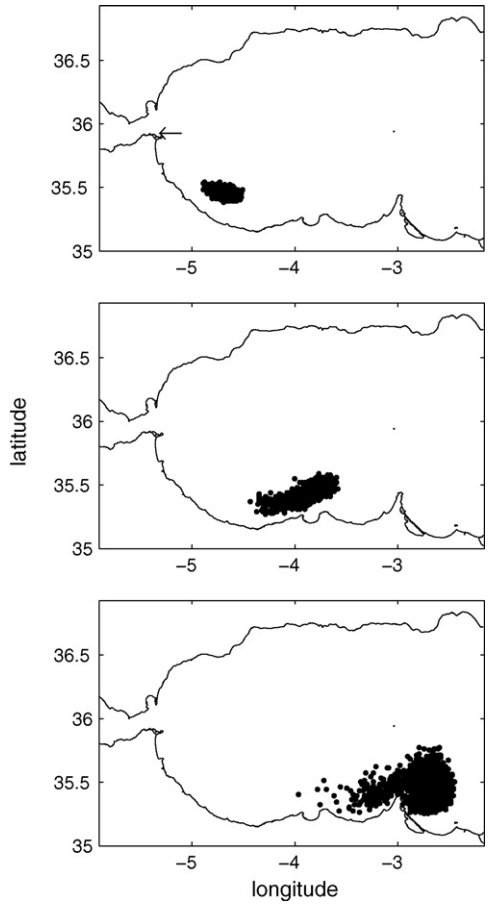

Fig. 12 – Snapshots showing the position of particles 22.5 (up), 25 (middle) and 90 (down) days after an instantaneous release of a stable chemical contaminant off Ceuta port, at the arrow position, with the coastal mode for residual circulation (usual winter conditions).

Finally an accident occurring in winter has been simulated. The instantaneous release was supposed to occur on 1 January 2005 at 0:00 h close to Ceuta harbour under calm wind. Results are presented in Fig. 12. It can be seen that the contaminant patch curves to the south and travels along the African coast. Nevertheless the speed of the patch is slower than when it is introduced in the Atlantic jet in the northern part of the sea (Fig. 6) during usual summer conditions. Now the patch travels some 82 km in 90 days, that results in an average speed of 1 cm/s. Similar results are obtained if the release occurs inside the Strait of Gibraltar.

4.3. *Model uncertainty and sensitivity*

It is difficult to assess the uncertainty of the model predictions. In the case of the dispersion model, an error is introduced because of the use of a first order accuracy advection scheme. However, Elliott and Clarke (1998) found no improvement in the results when a second order accuracy scheme was used to simulate the movement of surface drifters by the particle tracking technique. Moreover, in sea dispersion problems, the effects of turbulence will mask any small errors in the advection scheme. Also, Monte Carlo methods give an excellent approximation to the analytical solution of decay equations provided that enough particles are used (Periáñez and Elliott, 2002).

Of course, the main source of uncertainty is the calculation of currents by both hydrodynamic models. Although the output of both models has been compared with available measurements, the quality of solutions over the complete domain cannot be guaranteed. A wind forecast is also required to run the model in a real situation after an accident. Its accuracy cannot be assessed.

The model described in this paper is a tool designed to support the decision making process after a release of contamination in the sea, not for a theoretical study of the Alborán Sea physical oceanography. The difference is huge. Having a rapid response is essential in decision-making after an emergency and, of course, increasing computation speed implies that simplifications have to be carried out in the model. Particularly, it is required to have water currents fields computed in advance, so that it is not necessary to repeat hydrodynamic calculations (time consuming). Running time of the dispersion model is 5.4 s per day of simulation on a Pentium 4 PC, 3.2 GHz and 512 MB RAM (in case of a chemical spill, when some processes as buoyancy, beaching and evaporation are omitted). This is also in the case of an instantaneous release (constant number of particles during the complete simulation).

In the opinion of the author, the most dramatic problem is related with the residual circulation in the Alborán Sea. As already mentioned, the WAG is usually present in summer while the coastal mode is more likely in winter. However, there are transition episodes between both situations and it cannot be guaranteed that the WAG will always be present during the summer, for instance. Moreover, fluxes through the Strait of Gibraltar change and for a given situation (for instance coastal mode), water velocities may vary.

Let us imagine that an accident occurs just now. How do we run the model? In other words: is just now the WAG present? Which is the water inflow through the Strait just

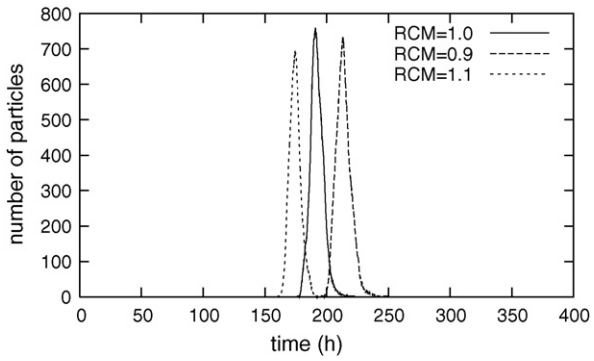

Fig. 13 – Time evolution of the number of particles at a point off the Málaga coast for the experiment in Fig. 6 and different values of the residual current modulator (RCM).

now? Presently it is not possible to have an answer. Thus, it is recommended to carry out calculations under the most probable conditions in a first guess: WAG in summer, coastal mode in winter. Additional simulations may then be carried out using the other circulation mode and different current modulators (to increase and reduce water velocities). This method will, at least, allow to estimate if there is any chance that a given sensible point (a coastal town for instance) is affected by contamination. As an example, the model sensitivity to the residual current modulator is shown in Fig. 13. The same experiment as in Fig. 6 has been repeated changing the modulator by 10%. Thus, 0.9 and 1.1 are used. The time evolution of the number of particles in a point off Málaga is presented in Fig. 13. Two main conclusions may be extracted. Firstly, the maximum number of particles (thus pollutant concentration) is not significantly affected by changes in the current magnitude. Secondly, the time of arrival of the contamination patch (or the time of maximum concentration) changes accordingly to the increase/decrease of the residual currents. Thus, the time of maximum concentrations ranges from 175 to 213 h, being 191 h for a current modulator equal to 1. This kind of sensitivity analysis can give an estimation of the lapse of time in which maximum concentrations may be expected and of the maximum response time to undertake countermeasures.

5. Conclusions

A particle-tracking model that simulates the dispersion of chemical pollutants and oil spills in the Strait of Gibraltar–Alborán Sea region has been developed. The contamination release is simulated by a number of particles whose paths are computed. Diffusion and decay are simulated by a Monte Carlo method. Specific processes for oil spills must also be included: buoyancy, evaporation and beaching of oil droplets. The currents required to calculate the advective transport are obtained from appropriate hydrodynamic models. Contaminant concentrations are obtained from the density of particles per water volume unit.

A 2D barotropic model is used to calculate tides over the domain. This model provides the tidal constants that are used by the dispersion model to reconstruct the tidal current at any time and position in the model domain. The residual circulation is obtained from a reduced gravity model. It was not possible to carry out a quantitative validation of this model, but computed currents are, at least, in qualitative agreement with observations available in the region. In particular, the main circulation features (the WAG and the coastal mode) are adequately reproduced by the model. Equations in both the barotropic and reduced gravity models are solved by standard explicit finite difference schemes.

The adopted approach (combining results from different hydrodynamic models to obtain the water circulation, together with the techniques of switching on and off the WAG and using the residual current modulator) has turned to be adequate for using it in a particle tracking dispersion model of an extremely complex basin. Of course, these techniques may be exported to other marine environments.

Some experiments concerning hypothetical releases in the region have been carried out. The average speed of a contamination patch released in the Strait of Gibraltar as it travels towards the eastern boundary of the domain is of some 9 and 1 cm/s for usual summer and winter conditions, respectively (existence of the WAG or coastal mode). If the accident occurs in the central part of the Alborán Sea, particles are trapped in the WAG, if present. The time required to complete a rotation has been estimated to be of the order of two months.

The simulation of a continuous release has been illustrated with the case of an oil spill occurring off Gibraltar port. The model predicts that a significant portion of the Spanish coast is contaminated.

Winds have a significant effect on the dispersion patterns in the area. Thus, dominant east winds tend to retain contaminants inside the Alborán Sea, also enhancing mixing along the transverse direction (north-south). The Spanish coast is more affected by contamination than under calm conditions. On the other hand, west winds produce a faster cleaning of the sea.

Acknowledgement

Work supported by the Research Project of Excellence RNM-419 *Técnicas Ultrasensibles para la Determinación de Radionucleidos en Muestras Ambientales*, Junta de Andalucía, Spain.

REFERENCES

Abril, J.M., Abdel-Aal, M.M., 2000. A modelling study on hydrodynamics and pollutant dispersion in the Suez Canal. Ecol. Model. 128, 1–17.

Autoridad Portuaria de la Bahía de Algeciras, 2006. Web site http://www.apba.es(in English and Spanish).

Arruda, W.Z., Nof, D., O'Brien, J.J., 2004. Does the Ulleung eddy owe its existence to β and norlinearities? Deep Sea Res. I 51, 2073–2090.

Béranguer, K., Mortier, L., Crépon, M., 2005. Seasonal variability of water transport through the Straits of Gibraltar, Sicily and Corsica, derived from a high-resolution model of the Mediterranean circulation. Prog. Oceanogr. 66, 341–364.

Cabello, J., 2003. Parque Natural del Estrecho, un nuevo futuro. Revista Medio Ambiente 43. Available on-line at http://www.juntadeandalucia.es/medioambiente (in Spanish).

Carreras, P.E., Menéndez, A.N., 1990. Mathematical simulation of pollutant dispersion. Ecol. Model. 52, 29–40.

Chern, C., Wang, J., 2005. Interactions of mesoscale eddy and western boundary current: a reduced gravity numerical model study. J. Oceanogr. 61, 271–282.
Cronk, J.K., Mitsch, W.J., Sykes, R.M., 1990. Effective modelling of a major inland oil spill in the Ohio River. Ecol. Model. 51, 161–192.
Cummins, P.F., Lagerloef, G.S.E., 2004. Wind-driven interannual variability over the northeast Pacific Ocean. Deep Sea Res. I 51, 2105–2121.
Dick, S., Schonfeld, W., 1996. Water transport and mixing in the North Frisian Wadden Sea. Results of numerical investigations. German J. Hydrogr. 48, 27–48.
Echevarría, F., García-Lafuente, J., Bruno, M., Gorsky, G., Goutx, M., González, N., García, C.M., Gómez, F., Vargas, J.M., Picheral, M., Striby, L., Varela, M., Alonso, J.J., Reul, A., Cozar, A., Prieto, L., Sarhan, T., Plaza, F., Jiménez-Gómez, F., 2002. Physical–biological coupling in the Strait of Gibraltar. Deep Sea Res. II 49, 4115–4130.
Elliott, A.J., 1986. Shear diffusion and the spread of oil in the surface layers of the North Sea. German J. Hydrogr. 39, 113–137.
Elliott, A.J., Clarke, S., 1998. Shallow water tides in the Firth of Forth. Hydrogr. J. 87, 19–24.
Elliott, A.J., Wilkins, B.T., Mansfield, P., 2001. On the disposal of contaminated milk in coastal waters. Mar. Pollut. Bull. 42, 927–934.
Elliott, A.J., 2004. A probabilistic description of the wind over Liverpool Bay with application to oil spill simulations. Estuar. Coast. Shelf Sci. 61, 569–581.
Gomez-Gesteira, M., Montero, P., Prego, R., Taboada, J.J., Leitao, P., Ruiz-Villareal, M., Neves, R., Perez-Villar, V., 1999. A two-dimensional particle-tracking model for pollution dispersion in A Coruña and Vigo Rias (NW Spain). Oceanol. Acta 22, 167–177.
Harms, I.H., Karcher, M.J., Dethleff, D., 2000. Modelling Siberian river runoff—implications for contaminant transport in the Artic Ocean. J. Mar. Syst. 27, 95–115.
Heburn, G.W., La Violette, P., 1990. Variations in the structure of the anticyclonic gyres found in the Alborán Sea. J. Geophys. Res. 95C2, 1599–1613.
Jacobi, C.M., Schaeffer-Novelli, Y., 1990. Oil spills in mangroves: a conceptual model based on long-term observations. Ecol. Model. 52, 53–59.
Jensen, T.G., 1998. Open boundary conditions in stratified ocean models. J. Mar. Syst. 16, 297–322.
Jusup, M., Gecek, S., Legovic, T., 2007. Impact of aquacultures on the marine ecosystem: modelling bethic carbon loading over variable depth. Ecol. Model. 200, 459–466.
Korotenko, K.A., Mamedov, R.M., Kontar, A.E., Korotenko, L.A., 2004. Particle-tracking method in the approach for prediction of oil slick transport in the sea: modelling oil pollution resulting from river input. J. Mar. Syst. 48, 159–170.
Kowalick, Z., Murty, T.S., 1993. Numerical Modelling of Ocean Dynamics. World Scientific, Singapore.
León-Vintró, L., Mitchell, P.I., Condren, O.M., Downes, A.B., Papucci, C., Delfanti, R., 1999. Vertical and horizontal fluxes of plutonium and americium in the western Mediterranean and the Strait of Gibraltar. Sci. Total Environ. 237, 77–91.
Manzella, G.M.R., Elliott, A.J., 1991. EUROSPILL: Mediterranean tidal and residual databases. Mar. Pollut. Bull. 22, 553–558.
Mañanes, R., Bruno, M., Alonso, J., Fraguela, B., Tejedor, L., 1998. Non-linear interaction between tidal and subinertial barotropic flows in the Strait of Gibraltar. Oceanol. Acta 21, 33–46.
Meyer, J.F.C.A., Diniz, G.L., 2007. Pollutant dispersion in wetland systems: mathematical modelling and numerical simulation. Ecol. Model. 200, 360–370.
Monte, L., Hakanson, L., Periáñez, R., Laptev, G., Zheleznyak, M., Maderich, V., Angeli, G., Koshebutsky, V., 2006. Experiences from a multi-model application to assess the behaviour of pollutants in the Dnieper–Bug Estuary. Ecol. Model. 195, 247–263.
Morales-Maqueda, M.A., Willmott, A.J., Darby, M.S., 1999. A numerical model for interdecadal variability of sea ice cover in the Greenland–Iceland–Norwegian Sea. Clim. Dynam. 15, 89–113.
Nav42, 1998. Report to the Maritime Safety Committee. International Maritime Organization. Available on line at http://www.navcen.uscg.gov/marcomms/imo/document.htm.
Nihoul, J., 1983/1984. A non-linear mathematical model for the transport and spreading of oil slicks. Ecol. Model. 22, 325–339.
Periáñez, R., Elliott, A.J., 2002. A particle tracking method for simulating the dispersion of non-conservative radionuclides in coastal waters. J. Environ. Radioactiv. 58, 13–33.
Periáñez, R., 1999. A three-dimensional σ-coordinate model to simulate the dispersion of radionuclides in the marine environment. Ecol. Model. 114, 59–70.
Periáñez, R., 2005a. An operative Lagrangian model for simulating radioactivity dispersion in the Strait of Gibraltar. J. Environ. Radioactiv. 84, 95–101.
Periáñez, R., 2005b. Modelling the Dispersion of Radionuclides in the Marine Environment. Springer-Verlag, Heidelberg.
Perkins, H., Kinder, T., La Violette, P., 1990. The Atlantic inflow in the western Alborán Sea. J. Phys. Oceanogr. 20, 242–263.
Preller, R.H., 1986. A numerical model study of the Alborán Sea gyre. Prog. Oceanogr. 16, 113–146.
Proctor, R., Flather, R.A., Elliott, A.J., 1994. Modelling tides and surface drift in the Arabian Gulf: application to the Gulf oil spill. Cont. Shelf Res. 14, 531–545.
Pugh, D.T., 1987. Tides, Surges and Mean Sea Level. Wiley, Chichester.
Reed, M., French, D.P., Calambokidis, J., Cubbage, J.C., 1989. Simulation modelling of the effects of oil spills on population dynamics of northern fur seals. Ecol. Model. 49, 49–71.
Riddle, A.M., 1998. The specification of mixing in random walk models for dispersion in the sea. Cont. Shelf Res. 18, 441–456.
Schonfeld, W., 1995. Numerical simulation of the dispersion of artificial radionuclides in the English Channel and the North Sea. J. Mar. Syst. 6, 529–544.
Tejedor, L., Izquierdo, A., Kagan, B.A., Sein, D.V., 1999. Simulation of the semidiurnal tides in the Strait of Gibraltar. J. Geophys. Res. 104, 13541–13557.
Tsimplis, M.N., Proctor, R., Flather, R.A., 1995. A two dimensional tidal model for the Mediterranean Sea. J. Geosphys. Res. 100, 16223–16239.
Tsimplis, M.N., Bryden, H.L., 2000. Estimations of the transports through the Strait of Gibraltar. Deep Sea Res. 47, 2219–2242.
Vargas-Yáñez, M., Plaza, F., García-Lafuente, J., Sarhan, T., Vargas, J.M., Velez-Belchi, P., 2002. About the seasonal variability of the Alborán Sea circulation. J. Mar. Syst. 35, 229–248.
Vázquez-Cuervo, J., Font, J., Martínez-Benjamín, J.J., 1996. Observations on the circulation of the Alborán Sea using ERS1 altimetry and sea surface temperature data. J. Phys. Oceanogr. 26, 1426–1439.
Vélez-Belchí, P., Vargas-Yáñez, M., Tintoré, J., 2005. Observation of a western Alborán gyre migration event. Prog. Oceanogr. 66, 190–210.
Werner, F.E., Cantos-Figueroa, A.Y., Parrilla, G., 1988. A sensitivity study of reduced-gravity flows with applications to the Alborán Sea. J. Phys. Oceanogr. 18, 373–383.
Wong, I., Swayne, D.A., Murthy, C.R., Lam, D.C.L., 1989. Fast graphical simulations of spills and plumes for application to the Great Lakes. Ecol. Model. 47, 161–173.